Journal of Organometallic Chemistry, 382 (1990) 201–224
Elsevier Sequoia S.A., Lausanne – Printed in The Netherlands
JOM 20563

The photochemistry of $M(CO)_4(\eta^4$-norbornadiene) complexes of group 6 transition metals (M = Cr, Mo, W) in low-temperature matrices *,**

Friedrich-Wilhelm Grevels *, Jürgen Jacke, Werner E. Klotzbücher, Kurt Schaffner

Max-Planck-Institut für Strahlenchemie, Stiftstraße 34–36, D-4330 Mülheim a.d. Ruhr (Federal Republic of Germany)

Richard H. Hooker and Antony J. Rest

Department of Chemistry, The University, Southampton, S09 5NH (United Kingdom)

(Received May 23rd, 1989)

Abstract

Photolysis of $M(CO)_4(\eta^4$-norbornadiene) group 6 metal complexes (**1**) in low-temperature matrices involves both loss of CO and cleavage of metal–olefin bonds to an extent depending on the metal and on the excitation wavelength. In inert matrices *mer*-$M(CO)_3(\eta^4$-NBD) (**2**, M = Cr), *fac*-$M(CO)_3(\eta^4$-NBD) (**3**, M = Cr, Mo, W), and *trans*-vacant $M(CO)_4(\eta^2$-NBD) (**7**, M = Mo) fragments are observed as primary photoproducts and characterized by means of IR and UV-visible spectroscopy. Secondary wavelength-dependent photoreactions of these fragments include partial regeneration of the starting material and reversible **2** ⇄ **3** photoisomerization (M = Cr). Experiments in ^{13}CO-doped matrices and with ^{13}CO-labelled starting material complement the characterization of **1**, **2**, and **3** (M = Cr). Remarkably, the *cis*-vacant $M(CO)_4(\eta^2$-NBD) fragment **9** could not be detected. For all three metals photolysis of **1** in the presence of excess carbon monoxide results in stepwise displacement of the NBD ligand, presumably via the initial formation of **7**, yielding $M(CO)_5(\eta^2$-NBD) (**4**) and $M(CO)_6$. The fragments **2**, **3**, and **7** can take up N_2 from the matrix environment to form *mer*-$M(CO)_3(\eta^4$-NBD)(N_2) (**5**, M = Cr), *fac*-$M(CO)_3(\eta^4$-NBD)(N_2) (**6**, M = Cr, Mo, W), and *trans*-$M(CO)_4(\eta^2$-NBD)(N_2) (**8**, M = Mo) as the major products. The relevance of these results with regard to the mechanism of the photocatalytic hydrogenation of norbornadiene is discussed.

---

* Dedicated to Professor Günther Wilke on the occasion of his 65th birthday.

** For preliminary accounts see ref. 1.

Introduction

The photochemical hydrogenation and hydrosilylation of dienes in the presence of group 6 metal carbonyls [2–14] is one of the better known examples for the use of UV-visible light in homogeneous catalysis. With conjugated dienes [2–4,6–11] the reactions result in specific *cis*-1,4-addition of H_2 or $HSiR_3$, eq. 1, yielding the corresponding *cis*-monoolefins [2–4,6,7,9–11] and allylsilanes [8,9], respectively. By contrast, hydrogenation of norbornadiene [3,5,12–14] yields two products, nortricyclene and norbornene, eq. 2.

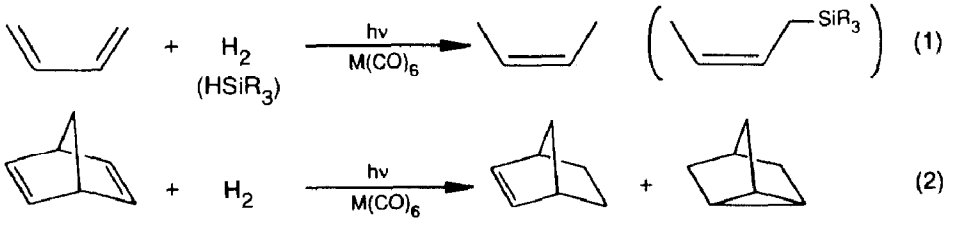

It has been shown that in the initial stages $M(CO)_4(\eta^4$-diene) complexes are formed which, however, are not the actual catalysts. Further irradiation is necessary to achieve catalytic activity by creating a vacant coordination site ready for binding H_2 or $HSiR_3$. Two different processes have been invoked in this context: photolytic $\eta^4 \rightarrow \eta^2$ dechelation of the diene on the one hand, and photodetachment of a CO group on the other hand. The latter reaction would imply that the $M(CO)_3$ moiety acts as the repeating unit in the catalytic cycle, which is in accord with the ability of $Cr(CO)_3(CH_3\text{-}CN)_3$ [15] and $Cr(CO)_3(\eta^6$-arene) complexes [16] to catalyse the hydrogenation of dienes under thermal conditions in the dark.

Our previous investigation into the photolytic behaviour of $Cr(CO)_4(\eta^4$-1,3-diene) complexes [17] in low-temperature matrices has demonstrated that indeed both of the two ligands, CO and diene, are displaced from the metal centre. However, the latter process becomes apparent only in neat carbon monoxide or in heavily CO-doped argon matrices. Under such conditions the (hitherto unobserved) $Cr(CO)_4(\eta^2$-1,3-diene) species is effectively trapped to form $Cr(CO)_5(\eta^2$-1,3-diene), which upon further irradiation yields $Cr(CO)_6$ as the ultimate product. The other process, photodetachment of CO, occurs selectively at an axial position, apparently the site adjacent to the "open" end of the diene, such that H_2 can be coordinated in an orientation suited for cis-1,4-hydrogenation of the diene (cf. I).

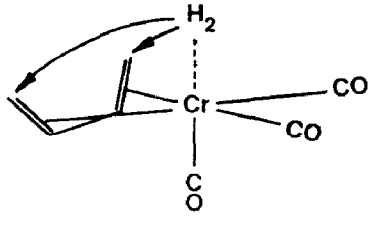

(I)

Evidence for the analogous reaction in the case of norbornadiene (NBD) comes from the photoinduced ^{13}CO incorporation into the axial positions of the

$M(CO)_4(\eta^4\text{-NBD})$ complexes II in solution [12,18]. This explains the photocatalytic formation of nortricyclene but not of norbornene, which is thought to involve $M(CO)_4(\eta^2\text{-NBD})$ as a key intermediate [5,12,14]. Surprisingly, the intermediacy of an equatorially vacant $M(CO)_3(\eta^4\text{-NBD})$ fragment has not been taken into consideration, neither in this context nor in that of the photochemical conversion of

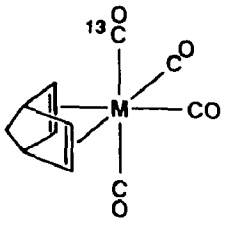

(II)

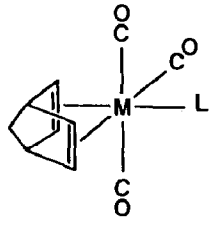

(III)

L = PR_3

L = olefin

$Cr(CO)_4(\eta^4\text{-NBD})$ into a *mer*-$M(CO)_3(PR_3)(\eta^4\text{-NBD})$ derivative (III) [19,20]. It should be noted that the same stereochemistry prevails in the photosubstitution of $W(CO)_4(\eta^4\text{-NBD})$ when an olefin is used as the incoming ligand, yielding *mer*-$W(CO)_3(\eta^4\text{-NBD})(\eta^2\text{-olefin})$ (III) [21].

In order to gain some information on the mechanistic implications of the above photoreactions, particularly on the possible primary photoproducts of the group 6 $M(CO)_4(\eta^4\text{-norbornadiene})$ complexes (**1**), we have investigated the low-temperature matrix photochemistry of these compounds. This work is related to complementary experiments in liquefied noble gases and flash photolysis studies with fast, time-resolved infrared detection aimed at the identification of key intermediates in the photocatalytic hydrogenation of norbornadiene [22,23].

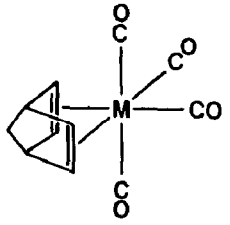

1a M = Cr
1b M = Mo
1c M = W

Experimental

Equipment and procedures. Details of the matrix isolation equipment have been described previously [24,25], including devices for controlling the temperature, flow of matrix gas (1.5–2 mmol h^{-1}), and metal complex deposition rate. Evaporation temperatures for the particular complexes (**1a**, 19 °C; **1b** 28 °C; **1c**, 37 °C) were adjusted to achieve guest/host ratios $\leqslant 1/1000$.

For narrow-band (ca. 13 nm) UV-visible irradiation a 900W Hg–Xe lamp (Hanovia 977-B 0010) was employed in combination with a Kratos-Schoeffel GM 252-1 monochromator ($\lambda/2$ radiation being removed by a short-wavelength cut-off filter), whereas for broad-band irradiation the light of a Philips HPK 125W mercury lamp was passed through the appropriate Schott cut-off filter.

UV-visible (Perkin Elmer 320 spectrometer) and IR spectra (Perkin Elmer 580 spectrometer, visible radiation from the sample beam being removed by an Oriel

germanium filter) were taken of the same matrix within a few minutes and stored on a Perkin Elmer 3600 data station.

Materials. Matrix gases ($\geq$ 99.99%; L'Air Liquide) were used as received. ^{13}C-labelled carbon monoxide was purchased from Promochem/Cambridge Isotope Laboratories (CLM-1845: ^{13}C 99%, ^{18}O < 1%). M(CO)$_4$(η^4-NBD) complexes (M = Cr [26], Mo [26] and W [27]) were prepared by thermal substitution of M(CO)$_6$ according to the published procedures. In case of the chromium complex the photochemical route (irradiation of 10 mM Cr(CO)$_6$ and 50 mM NBD in alkane solution, 81% yield) proved to be an advantageous alternative.

Results

*Photolysis of Cr(CO)$_4$(η^4-norbornadiene) (**1a**)*

(a) In methane and argon matrices. The CO stretching vibrational region of the infrared spectrum of **1a**, isolated in a methane matrix at 12 K, is displayed in Fig. 1A. It exhibits the four-band pattern characteristic for a complex of this type with a C_{2v} M(CO)$_4$ moiety. In various matrix materials slightly different band positions are observed, with a general high frequency shift in going from CH_4 and CO to N_2

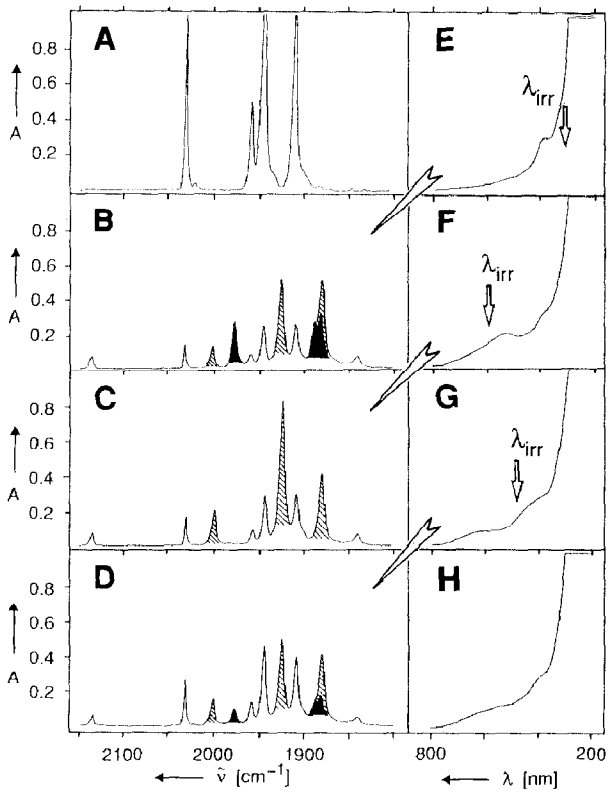

Fig. 1. Infrared and electronic absorption spectra from an experiment with Cr(CO)$_4$(η^4-norbornadiene) (**1a**), isolated in a methane matrix at 12 K: (A/E) after deposition; (B/F) after 10 min irradiation with λ 313 nm; (C/G) after subsequent 2 min irradiation with λ 579 nm; (D/H) after subsequent 40 min irradiation with λ 491 nm. Hatched and black marked bands are assigned to *mer*- and *fac*-Cr(CO)$_3$(η^4-norbornadiene) (**2a** and **3a**), respectively.

and Ar (Table 1). The electronic absorption spectrum (Fig. 1E) exhibits a maximum at 390 nm and a tail absorption towards longer wavelengths, responsible for the yellow colour of the complex.

Upon irradiation at wavelengths ranging from ca. 400–250 nm the four bands in the IR spectrum of **1a** gradually diminish while several new features grow in at 2135.5, 2000, 1975.5, 1925, 1886.5 (sh), 1879, and 1838.5 cm^{-1}. Examplarily Fig. 1B shows the result of altogether 10 min irradiation at λ 313 nm, whereupon 85% of **1a** have disappeared. The band at 2135.5 cm^{-1} is readily attributed to liberated CO, whereby the intensity of this feature ($\epsilon_{CO} \approx 400$ l mol^{-1} cm^{-1}, in methylcyclohexane glass) [28] accounts for the dissociation of ca. 1 mol CO from **1a** (ε 6320 l mol^{-1} cm^{-1} at 2032.5 cm^{-1}, in n-hexane solution). Thus, at this stage already, it is evident that loss of CO, most probably with formation of $Cr(CO)_3(\eta^4\text{-NBD})$, is the

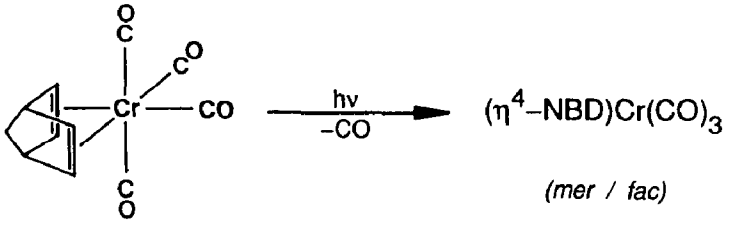

(3)

1a **2a / 3a**

predominant, if not exclusive, primary photoreaction of **1a**, eq. 3. As will be substantiated below on the basis of the other new IR bands, this fragment [29*] exists in two isomeric forms with a *mer*- and *fac*-$Cr(CO)_3$ skeleton, respectively.

Concomitant with the above IR spectral changes a broad new feature appears around 520 nm in the visible region of the electronic spectrum (Fig. 1F). Subsequent irradiation with λ 579 nm results in partial depletion of the absorption in this region (Fig. 1G) and in substantial changes in the IR spectrum as well (Fig. 1C). The latter indicates partial recovery of the starting material together with an increase of the hatched three-band pattern, designated as **2a**, at the expense of the band at 1975.5 cm^{-1} and the shoulder at 1886.5 cm^{-1}, which disappear completely and thus are assigned to a different fragment, **3a**. It is obvious from the intensity changes at 1879 cm^{-1} that at this position a third band of **3a** is overlapping with one of **2a**. This is clearly borne out by computer-assisted subtraction of the spectra, as shown in Fig. 2. Subsequent irradiation with λ 491 nm causes partial recovery of **3a** and, again, of the starting material **1a** at the expense of the bands associated with **2a** (Fig. 1D). Based on the concomitant changes in the electronic absorption spectra we conclude that the two long-wavelength features at 450 nm and 620 nm in Fig. 1G are associated with **2a**, while the maximum emerging near 520 nm (Figs. 1F and 1H) has to be attributed to **3a**.

The readily occurring partial recovery of the starting material **1a** in both of the above long-wavelengths irradiations is in accord with the assumption that the chromium(η^4-norbornadiene) moiety is not affected in either of the two species **2a** and **3a**, i.e., we are dealing with two isomeric $Cr(CO)_3(\eta^4\text{-NBD})$ fragments. Both of

* Reference number with asterisk indicates a note in the list of references.

Table 1

Infrared CO stretching vibrational data (cm^{-1}) and UV-visible absorptions (nm) of $M(CO)_4(\eta^4$-norbornadiene) complexes (M = Cr, Mo, W) and their photoproducts in low-temperature matrices

Complex	Matrix	IR				UV-visible
$Cr(CO)_4(\eta^4$-NBD)	Ar	2037.5	1964	1950.5	1918.5	390
(1a)	CH_4	2031.5	1957.5	1944.5	1908.5	
	N_2	2036	1963	1947	1916	390
	CO	2031.5	1958	1943	1910	390
	Ar/CO (5/1)	2031	1956	1942	1908.5	395
	Ar/N_2 (10/1)	2036	1962.5	1949	1917	395
$Mo(CO)_4(\eta^4$-NBD)	CH_4	2045	1959	1906.5		270(sh), 295, 360
(1b)	Ar	2050	1964	1917.5		270, 295, 360
	CO	2046	1956.5	1908		275, 300, 365
	Ar/CO (10/1)	2047	1960.5	1911.5		
	N_2	2048.5	1959.5	1913		270, 297, 365
	Ar/N_2 (10/1)	2049	1962.5	1915.5		275, 295, 360
$W(CO)_4(\eta^4$-NBD)	Ar	2050.5	1963	1914.5		250, 273, 295(sh), 370
(1c)	CH_4	2044.5	1957.5	1903		
	CO	2044.5	1955.5	1903.5		
	N_2	2048.5	1988.5	1910		
mer-$Cr(CO)_3(\eta^4$-NBD)	Ar	2005.5	1932	1894.5		450, 620
(2a)	CH_4	2000	1925	1880		450, 620
	Ar/CO (5/1)	1999.5	1924	(~1880) [a]		
	Ar/N_2 (10/1)	(2004)	1930	1892		
mer-$Mo(CO)_3(\eta^4$-NBD)	Ar	(2024 or 2007.5) [c]	1950.5	(~1900) [a]		
(2b)						
fac-$Cr(CO)_3(\eta^4$-NBD)	Ar	1982.5	1895	1891		520
(3a)	CH_4	1975.5	1886.5	1878		
	Ar/CO (5/1)	1976	(~1880)			
	Ar/N_2 (10/1)	1981.5	(~1888)			

fac-$Mo(CO)_3(\eta^4$-NBD)	CH_4	1981	1893	1882		400(sh)
(3b)	Ar	1988	1900	1893.5		430
	Ar/N_2 (10/1)	1986.5	1899.5	1891.7		
	Ar/CO (10/1)	1985.5	1889(br)			430
fac-$W(CO)_3(\eta^4$-NBD)	Ar	1988	1906.5	1890		290(sh), 433
(3c)	CH_4	1981	(~1899) [a]	1877.5		400
$Cr(CO)_5(\eta^2$-NBD)	CO	2068	1957	1946		370(sh)
(4a)						
$Mo(CO)_5(\eta^2$-NBD)	CO	2078	(~1942)			
(4b)	Ar/CO (10/1)	2080.5	(–) [a]			
$W(CO)_5(\eta^2$-NBD)	CO	2078.5	(~1942,sh) [a]			
(4c)						
mer-$Cr(CO)_3(\eta^4$-NBD)(N_2)	N_2	2182.5 [b]	2004	1938.5		
(5a)	Ar/N_2 (10/1)	2176.5 [b]	2004.5	1941.5		
fac-$Cr(CO)_3(\eta^4$-NBD)(N_2)	N_2	2207.5 [b]	1988.5	(~1902,br)		
(6a)	Ar/N_2 (10/1)	2201.5 [b]	1990	1904		
fac-$Mo(CO)_3(\eta^4$-NBD)(N_2)	N_2	2229 [b]	1991	1926.5	1899	
(6b)						
fac-$W(CO)_3(\eta^4$-NBD)(N_2)	N_2	2211.5 [b]	1993	1931	1898	
(6c)						
trans-$Mo(CO)_4(\eta^2$-NBD)	CH_4	1898.5				260(sh), ~500(br)
(7b)	Ar	1903				260, ~430(br), ~560(br)
	Ar/CO (10/1)	1899.5				
	Ar/N_2 (10/1)	1901.5				
trans-$Mo(CO)_4(\eta^2$-NBD)(N_2)	N_2	2196.5 [b]	1930			
(8b)	Ar/N_2 (10/1)	2193 [b]	1932.5			
trans-$W(CO)_4(\eta^2$-NBD)(N_2)	N_2	2179 [b]	(~1923)			
(8c)						

[a] Overlapping with other spectral features. [b] ν(N≡N). [c] Either of the two bands can be attributed to **2b**, the other remains unassigned.

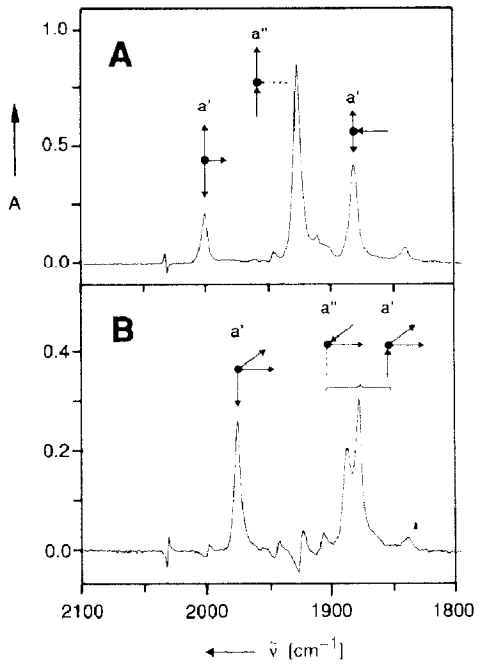

Fig. 2. Infrared CO stretching vibrational patterns of (A) *mer*-$Cr(CO)_3(\eta^4$-norbornadiene) (**2a**) and (B) *fac*-$Cr(CO)_3(\eta^4$-norbornadiene) (**3a**), obtained by computer-assisted subtraction of spectra displayed in Fig. 1. (A): spectrum 1C–(0.17 × spectrum 1A). (B): spectrum 1B–(0.61 × spectrum 1C)– (0.05 × spectrum 1A). (The interference-free bands at 2031.5 and 2000 cm^{-1} were used as subtraction standards).

the two possible structures, with a vacant coordination site in either an axial or an equatorial position, possess C_s symmetry. However, in the latter case, with a *mer*-$Cr(CO)_3$ skeleton, a distinct progression of the relative intensities of the three CO stretching vibrational modes in the order I(in phase a′) < I(out-of-phase a′) < I(a″) can be expected [21,30,31], whereas in the axially vacant fragment with a *fac*-$Cr(CO)_3$ geometry the totally symmetric, high-frequency a′ mode and the two low-frequency modes should exhibit similar intensities [30]. Thus, the assignment of the *mer*- and *fac*-$Cr(CO)_3(\eta^4$-NBD) structures to the two species **2a** and **3a**, respectively, on the basis of the intensity patterns displayed in Fig. 2 is straightfor-

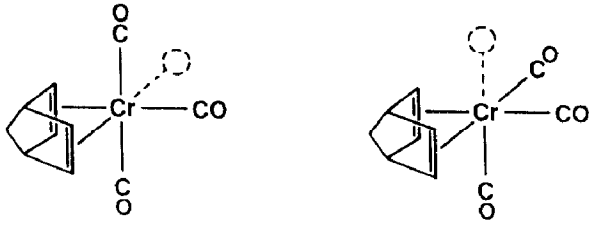

2a [*mer*-$Cr(CO)_3$ skeleton]

3a [*fac*-$Cr(CO)_3$ skeleton]

ward. The only IR feature not properly assignable to a particular species is the weak band at 1838.5 cm^{-1}. Considering the position of this band one might speculate about a trace amount of $Cr(CO)_2(\eta^4$-NBD), resulting from secondary photolysis of either **2a** or **3a**. However, by analogy with the two tricarbonyl fragments, such a

species is expected to diminish by taking up liberated CO upon long-wavelength irradiation, which is not observed.

The starting material (**1a**) itself does not show any reaction upon irradiation at either of the two longer wavelengths, 579 nm and 491 nm. Hence it follows that the photointerconversion of the isomers **2a** and **3a** at these wavelengths does not involve the re-formation and subsequent photolysis of **1a** as intermediate steps, but rather takes place by direct skeletal rearrangement [32*] in either direction, eq. 4, with re-formation of some **1a** occurring simultaneously as a side reaction.

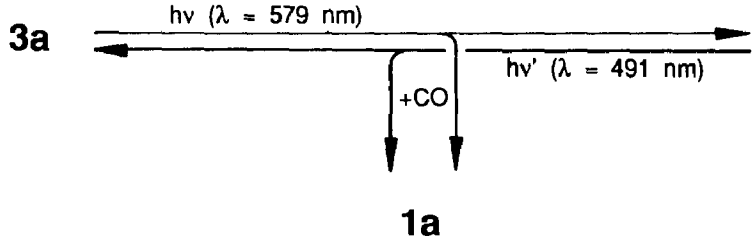

(4)

In argon matrices (cf. Table 1) the photolysis of **1a** at λ 313 nm (and at λ 289 nm as well) takes essentially the same course as described above, including the selective interconversion of the two isomeric fragments **2a** and **3a** upon subsequent irradiation at the longer wavelengths.

Quantitative evaluations of these experiments indicate some variation of the product ratio with the excitation wavelength. The relative molar IR absorbances of the starting material and the two fragments are slightly different in methane [$\epsilon_{1a}(2031.5\ cm^{-1})/\epsilon_{2a}(2000\ cm^{-1})/\epsilon_{3a}(1975.5\ cm^{-1}) \approx 3/1/3$] and argon matrices [$\epsilon_{1a}(2037.5\ cm^{-1})/\epsilon_{2a}(2005.5\ cm^{-1})/\epsilon_{3a}(1982.5\ cm^{-1}) \approx 2.5/1/3$]. However, these data represent average values whose error is in the order of 15–20%. This is due to some deficits in the material balances (cf. the unidentified minor side product mentioned above) and, likewise important, some changes in the bandshapes and halfwidths, which are difficult to account for on a quantitative level. Nevertheless, despite such reservations concerning the accuracy, careful monitoring of the appearance of **2a** and **3a** upon monochromatic photolysis of **1a** provides some interesting information. Thus we note that the *mer/fac* product ratio not only depends on the wavelength of irradiation, but also may change in the course of a particular experiment as the conversion of **1a** proceeds. At λ 289 nm in argon (Fig. 3) for example, the **2a** /**3a** ratio decreases gradually from an initial value of 3/1 (at ca. 10% conversion of **1a**) to 1.5/1 (at ca. 70% conversion of **1a**), thus indicating that secondary *mer* → *fac* photoisomerization takes place to a significant extent as the starting material disappears and, consequently, exercises a diminishing internal light filter effect. Regarding the initial *mer/fac* product ratios ($\leqslant$ 20% conversion of **1a**) at different wavelengths we note that the above value at 289 nm (3/1) represents the maximum. It drops in either direction, viz., sharply to ca. 0.8/1 at 253 nm and slightly to 2/1 and 1.3/1 at 313 and 404 nm, respectively.

Taking advantage of the recently developed [33*] route to the mono-(^{13}CO)-labelled derivative of **1a**, $Cr(CO)_3(^{13}CO)(\eta^4\text{-NBD})$, we were able to generate and characterize the respective mono-labelled fragments of type **2a** and **3a**. The starting material used in this experiment contains both (ax-^{13}CO)-**1a** and (eq-^{13}CO)-**1a**, together with ca. 50% unlabelled **1a** [33*]. The CO stretching vibrational region in

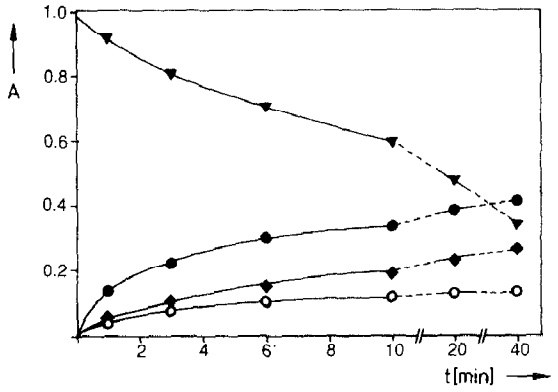

Fig. 3. Plot of IR absorbance data vs. time showing the formation of **2a** (● at 2005.5 cm^{-1}, ○ at 1932 cm^{-1}) and **3a** (◆ at 1982.5 cm^{-1}) upon irradiation of **1a** (▼ at 2037.5 cm^{-1}) at λ 289 nm in an argon matrix. Note that the ●/○ ratio remains constant (3±0.2) while the ◆/○ and ◆/● ratios gradually increase as the conversion of **1a** proceeds.

the infrared spectrum of this material, isolated in a methane matrix at 12 K, is displayed in Fig. 4A. The observed data, collected in Table 2, are used to calculate the CO-factored force field parameters, which are in general agreement with the data previously extracted from the solution spectra of $M(CO)_4(\eta^4\text{-NBD})$ (M = Cr,

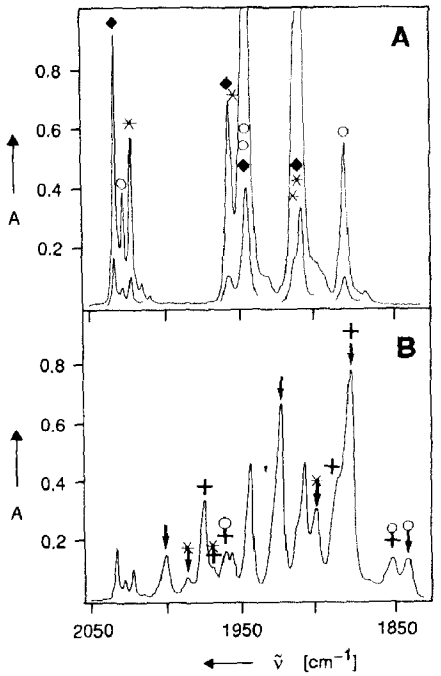

Fig. 4. Infrared spectra in the ν(CO) region from an experiment with a ^{13}CO-enriched sample of $Cr(CO)_4(\eta^4\text{-NBD})$ [33*] containing unlabelled **1a** (◆), ax-^{13}CO-**1a** (*), and eq-^{13}CO-**1a** (○) isolated in a methane matrix at 12 K: (A) after deposition; (B) after 10 min irradiation with λ 313 nm, showing the formation of *mer*-$Cr(CO)_3(\eta^4\text{-NBD})$ (**2a**, ↓), ax-^{13}CO-**2a** (↕), eq-^{13}CO-**2a** (♀), *fac*-$Cr(CO)_3(\eta^4\text{-NBD})$ (**3a**, +), ax-^{13}CO-**3a** (ǂ), and eq-^{13}CO-**3a** (♀). For assignments of overlapping bands cf. Table 2.

Table 2

Infrared CO stretching vibrational data [a] (cm^{-1}) and force field parameters [b] ($N\ m^{-1}$) of **1a**, **2a**, **3a**, and the respective ^{13}CO-labelled derivatives

Complex		Observed [a]	Calculated [b]
$Cr(CO)_4(\eta^4$-NBD)	A_1	2033.1	2033.0
(**1a**, C_{2v})	A_1	1957.6	1957.4
	B_1	1945.6	1945.0
	B_2	1909.6	1909.1
(ax-^{13}CO)-**1a**	A′	2022.2	2022.3
(C_s)	A′	[c]	1955.0
	A′	1913.3(sh)	1914.1
	A″	[d]	1909.1
(eq-^{13}CO)-**1a**	A′	2027.5	2027.5
(C_s)	A′	[c]	1947.6
	A″	[d]	1945.0
	A′	1880.5	1881.1
mer-$Cr(CO)_3(\eta^4$-NBD)	A′	2000.8	2000.8
(**2a**, C_s)	A″	1926.0	1926.0
	A′	1879.9	1879.9
(ax-^{13}CO)-**2a**		1986.0	1985.9
(C_1)		1901.3	1901.4
		[c]	1875.6
(eq-^{13}CO)-**2a**	A′	[c]	1998.1
(C_s)	A″	[d]	1926.0
	A′	1840.4	1840.5
fac-$Cr(CO)_3(\eta^4$-NBD)	A′	1975.5	1975.3
(**3a**, C_s)	A′	1887.4	1887.4
	A″	1878.0	1878.0
(ax-^{13}CO)-**3a**	A′	(1970) [e]	1969.4
(C_s)	A″	[d]	1878.0
	A′	[c]	1850.9
(eq-^{13}CO)-**3a**		1961.5	1961.7
(C_1)		[c]	1886.2
		1850.0	1850.1

[a] Methane matrix, 12 K; the data observed for unlabelled **1a**, **2a**, and **3a** agree with those from other experiments in methane matrices (Table 1) within experimental error (1–1.5 cm^{-1}). [b] CO force field parameters ($N\ m^{-1}$): **1a**, $k_{ax} = 1578.4$, $k_{eq} = 1530.7$, $k_{ax,eq} = 28.8$, $k_{eq,eq} = 58.3$, $k_{ax,ax} = 50.2$; **2a**, $k_{ax} = 1550.1$, $k_{eq} = 1443.1$, $k_{ax,eq} = 36.8$, $k_{ax,ax} = 51.6$; **3a**, $k_{ax} = 1465.1$, $k_{eq} = 1487.5$, $k_{ax,eq} = 38.1$, $k_{eq,eq} = 62.8$. [c] Overlapping with more prominent bands. [d] Coincident with other bands. [e] Barely observable.

Mo, W) [34*]. Irradiation of this material at λ 313 nm, by analogy with the photolysis of unlabelled **1a** (vide supra), results in the formation of **2a** and **3a** and of the respective mono-(^{13}CO)-labelled species as well (Fig. 4B, Table 2). The bands associated with (ax-^{13}CO)/(eq-^{13}CO)-**2a** are readily distinguished from those of (ax-^{13}CO)/(eq-^{13}CO)-**3a** by monitoring the changes in intensities occurring (i) upon subsequent selective irradiations at longer wavelengths (610, 579, 546 nm) leading to *fac* → *mer* photoisomerization of the $Cr(CO)_3(\eta^4$-NBD) fragment (by analogy with

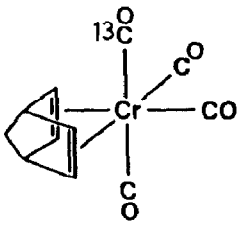

ax-^{13}CO-**1a**

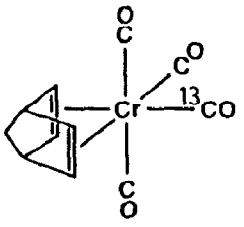

eq-^{13}CO-**1a**

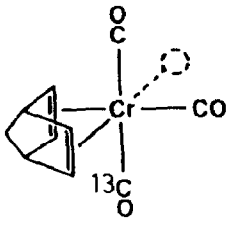

ax-^{13}CO-**2a**

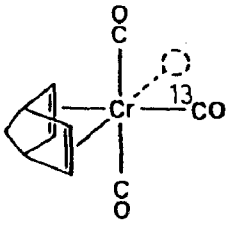

eq-^{13}CO-**2a**

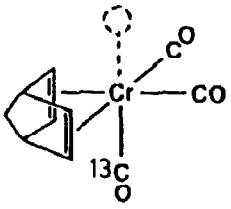

ax-^{13}CO-**3a**

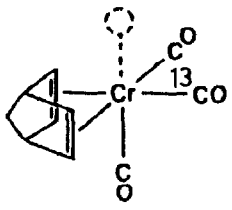

eq-^{13}CO-**3a**

Fig. 1C) and (ii) upon irradiation at 435 nm which results in *mer* → *fac* rearrangement (by analogy with 491 nm irradiation, Fig. 1D). The force field parameters of both species, **2a** and **3a**, are calculated from the observed data collected in Table 2.

Comparing the data sets of the two fragments **2a** and **3a** with those of the parent tetracarbonyl we note that loss of a CO group from **1a** in general results in the expected decrease in both principal force constants, but with pronounced specific effects. In detail: detachment of an axial CO group, yielding **3a**, reduces k_{ax} by as much as 113 N m^{-1} and k_{eq} by only 43 N m^{-1}. The analogous effects resulting from loss of an equatorial CO group, yielding **2a**, are somewhat smaller and here it is k_{eq} which is predominantly affected.

(b) In matrices containing carbon monoxide or dinitrogen. Photodetachment of CO has been the only primary photoreaction of $Cr(CO)_4(\eta^4$-NBD) observable in

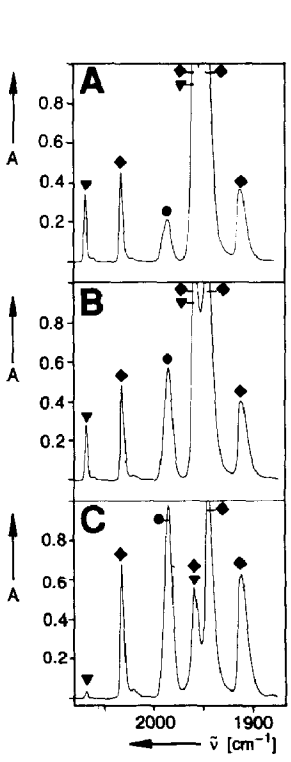

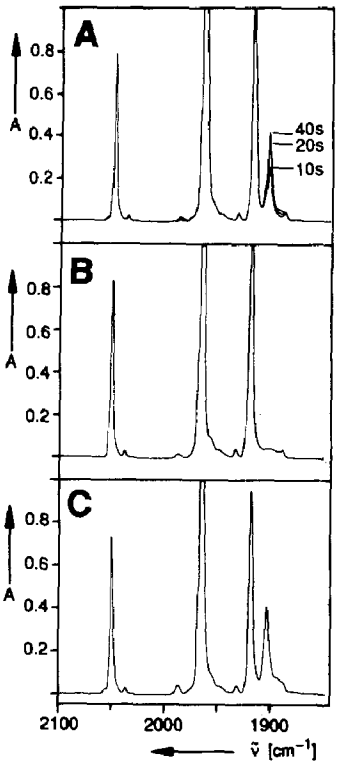

Fig. 5. Infrared spectra in the ν(CO) region from an experiment with $Cr(CO)_4(\eta^4$-norbornadiene) (**1a**, ◆), isolated in a carbon monoxide matrix at 12 K: (A) after 16 h irradiation through a cut-off filter with $\lambda \geqslant 435$ nm, showing the formation of $Cr(CO)_5(\eta^2$-norbornadiene) (**4a**, ▼) and $Cr(CO)_6$ (●); (B) after subsequent 30 min irradiation through a cut-off filter with $\lambda \geqslant 400$ nm; (C) after subsequent 1 min irradiation with λ 365 nm.

Fig. 6. Infrared spectra in the ν(CO) region from an experiment with $Mo(CO)_4(\eta^4$-NBD) (**1b**), isolated in an argon matrix at 12 K: (A) after deposition and 10, 20, and 40 s irradiation with λ 365 nm, showing the formation of *trans*-$Mo(CO)_4(\eta^2$-NBD) (**7b**); (B) after subsequent 1 min irradiation with λ 546 nm; (C) after subsequent 30 s irradiation with λ 365 nm.

the above experiments. No evidence could be found for the alternative process, dechelation of the η^4-coordinated norbornadiene ligand yielding $Cr(CO)_4(\eta^2$-NBD), possibly because of rapid $\eta^2 \rightarrow \eta^4$ chelate re-formation. If so, such a species might be trapped in a matrix environment containing other potential ligands, such as CO or N_2, which could occupy the vacant coordination site rapidly enough to prevent re-formation of the chelate complex.

Indeed, in a carbon monoxide matrix photolysis of $Cr(CO)_4(\eta^4$-NBD) (**1a**) results in the formation of $Cr(CO)_5(\eta^2$-NBD) (**4a**) and, ultimately, $Cr(CO)_6$. Upon irradiation with $\lambda \geqslant 435$ nm into the long-wavelength tail of the UV-visible absorption of **1a**, the 2031.5 cm^{-1} and 1910 cm^{-1} ν(CO) bands of the tetracarbonyl complex gradually diminish, whereas the absorptions near 1958 and 1943 cm^{-1} increase in intensity. Furthermore, new bands emerge at 2068 and 1984 cm^{-1} (Fig. 5A). The latter feature is readily assigned to $Cr(CO)_6$, while the former is part of a three-band pattern (2068, 1957, and 1946 cm^{-1}), as shown by computer-assisted subtraction of spectra at different stages of the experiment. Comparison with

various $M(CO)_5(\eta^2$-olefin) spectra [28,35–37] establishes the assignment of this species to $Cr(CO)_5(\eta^2$-NBD) (**4a**) [38*]. After several hours of irradiation with $\lambda \geq 435$ nm the progress of the reaction ceases when ca. 50% of **1a** is converted into the two photoproducts. Concomitantly, the maximum at 390 nm in the electronic absorption spectrum of **1a** flattens, while a new shoulder emerges at slightly shorter wavelength, 370 nm, reasonably attributable to **4a**. Upon further irradiation, but through a shorter wavelength cut-off filter ($\lambda \geq 400$ nm), the IR bands of **4a** gradually diminish. After 30 min ca. 20% of **4a** has disappeared with almost exclusive formation of $Cr(CO)_6$ (Fig. 5B). Much faster conversion of **4a** (nearly complete after 1 min) occurs upon irradiation at 365 nm. However, at this wavelength photodetachment of CO with regeneration of the tetracarbonyl complex **1a** clearly predominates by a factor of 2.5 over η^2-norbornadiene displacement leading to $Cr(CO)_6$ (Fig. 5C). Similar results are obtained when **4a**, subsequent to its photochemical generation from **1a** with $\lambda \geq 435$ nm, is irradiated at λ 313 nm.

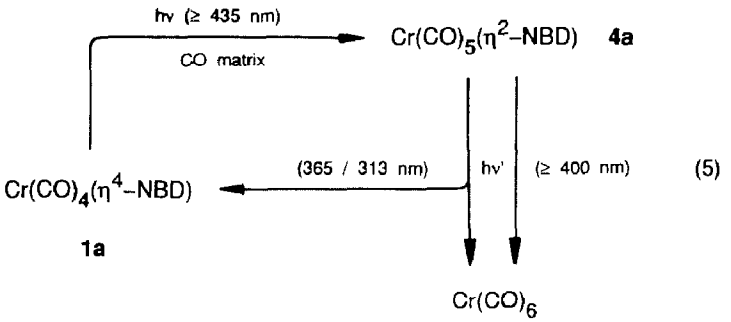

It is evident from these experiments that under suitable conditions, by analogy with the photochemical behaviour of $Cr(CO)_4(\eta^4$-1,3-diene) compounds [17], stepwise photosubstitution of the norbornadiene ligand in **1a** by two CO groups, eq. 5, plays a significant role. However, accumulation of the intermediate product, $Cr(CO)_5(\eta^2$-NBD) (**4a**), requires selective irradiation into the long-wavelength tail absorption of **1a**. This is demonstrated by the photolysis of **1a** in an Ar-CO (5/1) matrix with λ 365 and 313 nm, which yields $Cr(CO)_6$, albeit to a minor extent compared with the experiment in a neat CO matrix, while **4a** does not show up. Moreover, the dilution with argon uncovers the simultaneous photolytic loss of CO as manifested by the appearance of both *mer*- and *fac*-$Cr(CO)_3(\eta^4$-NBD) fragments, **2a** and **3a** (Table 1). In matrices containing only 5% CO the formation of $Cr(CO)_6$ is almost negligible.

In the presence of ^{13}CO photogenerated **2a** and **3a** take up the labelled CO group from the matrix environment. Thus, in a ^{13}CO–CH_4 (1/16) matrix photolysis of **1a** at λ 313 nm not only yields the two $Cr(CO)_3(\eta^4$-NBD) fragments **2a** and **3a** but, after 30–40% conversion of **1a** (ca. 1 min), ν(CO) bands begin to grow in which are characteristic of ^{13}CO-labelled **1a**, **2a**, and **3a** (cf. Table 2). After 2 min of irradiation (65% conversion of **1a**) bands at 2027 cm^{-1} (eq-^{13}CO-**1a**), 2021.5 cm^{-1} (ax-^{13}CO-**1a**), ca. 1900 cm^{-1} (sh, ax-^{13}CO-**2a**), 1850 cm^{-1} (ax/eq-^{13}CO-**3a**), and 1839 cm^{-1} (eq-^{13}CO-**2a**) are clearly discernible, while other absorptions associated with these species overlap with those of the predominant, unlabelled complexes. Upon subsequent irradiation at λ 579 nm both **3a** and ax/eq-^{13}CO-**3a** disappear with concomitant reformation of **1a** and further formation of eq-^{13}CO-**1a**, ax-^{13}CO-

1a, and (to a minor extent) **3a**; a weak band at 2014 cm^{-1} indicates the appearance of doubly ^{13}CO-labelled **1a**. Accordingly, subsequent irradiation at 491 nm converts a substantial amount of both unlabelled and ^{13}CO-labelled **3a** into **1a**, eq-^{13}CO-**1a**, and ax-^{13}CO-**1a**, while *mer* → *fac* fragment rearrangement is a minor process. Further photolysis at 313 nm leads to a complex mixture of species with increasing degree of ^{13}CO incorporation into the various CO positions of **1a**, **2a**, and **3a**.

In a dinitrogen matrix $Cr(CO)_4(\eta^4\text{-NBD})$ (**1a**) loses carbon monoxide (2140 cm^{-1}) and is rapidly converted into a mixture of N_2-containing complexes, as indicated by the appearance of several bands in the $\nu(N{\equiv}N)$ region of the infrared spectrum. After 6 min of irradiation at λ 313 nm ca. 70% of **1a** has disappeared. Two of the products, *mer*- and *fac*-$Cr(CO)_3(\eta^4\text{-NBD})(N_2)$ (**5a**, **6a**), are readily

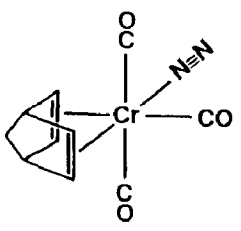

5a

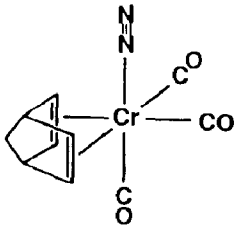

6a

identified on the basis of their infrared data (Table 1). The lower frequency of the $\nu(N{\equiv}N)$ vibration of **5a**, compared with that of **6a**, is in accord with the N_2 ligand having an olefin rather than a CO group in trans position. The η^2-(C=C) unit, being a single-faced π-acceptor ligand, competes less effectively for metal(d_π) electron density than does a CO group. Consequently, metal(d_π) → $N_2(\pi^*)$ back donation is stronger in the case of **5a**, which implicates a lower $\nu(N{\equiv}N)$ frequency. The assignment of other, weaker absorptions in the $\nu(N{\equiv}N)$ region (2187, sh; 2156 cm^{-1}) remains somewhat ambiguous since the corresponding CO stretching vibrational features around 1890–1920 cm^{-1} are not clearly resolved and separated from others. It seems possible that two species, *trans*-$Cr(CO)_4(\eta^2\text{-NBD})(N_2)$ (2187 and ca. 1908 cm^{-1}; cf. data of the analogous Mo complex **8b**, Table 1) and *trans*-$Cr(CO)_2(\eta^4\text{-NBD})(N_2)_2$ (2156 and ca. 1893 cm^{-1}), in addition to **5a** and **6a**, are present in the reaction mixture. Two minor $\nu(CO)$ features at 2080 and 2062 cm^{-1} remain unassigned. The electronic absorption spectrum, after 70% conversion of **1a**, shows a new, but poorly resolved shoulder appearing around 350 nm and a moderate increase in absorbance around 450 nm. However, it is not possible to assign these spectral changes to a particular product. Subsequent irradiation with λ 435 nm results in the recovery of some **1a** and, to a minor extent, the formation of **5a** at the expense of the *fac* isomer **6a**, the IR bands of which diminish by a factor of 3 after 40 min.

Similar irradiation of **1a** at λ 313 nm, but in an $Ar{-}N_2$ (10/1) matrix, again results in loss of CO (2138.5 cm^{-1}) from both the equatorial and the axial positions, yielding the *mer*- and *fac*-N_2 substituted derivatives (**5a**, **6a**) together with the respective coordinatively unsaturated species **2a** and **3a**. Although some of the characteristic IR bands (Table 1) are overlapping, unambiguous assignments are possible on the basis of the spectral changes occurring upon subsequent irradiation at longer wavelengths. With λ 579 nm the unsaturated *fac* species **3a** disappears largely, with formation of the *fac*-N_2 complex **6a**, some **2a** and **5a** and even a trace

regeneration of the starting material **1a**. Subsequent irradiation with λ 491 nm results in re-formation of the unsaturated *fac* species **3a**, mainly at the expense of the *mer* isomer **2a**, and in a further increase of the bands associated with **1a**, **5a**, and **6a**.

Photolysis of $Mo(CO)_4(\eta^4$-norbornadiene) (1b)

The photochemistry of **1b** differs from that of the analogous chromium compound, described above, in two essential points. First of all, loss of CO from the equatorial position yielding a fragment of type **2**, *mer*-$Mo(CO)_3(\eta^4$-NBD), is almost negligible at any wavelength. Secondly, there is a much more pronounced wavelength dependence in so far that formation of the type **3** fragment, *fac*-$Mo(CO)_3(\eta^4$-NBD), resulting from axial CO photodetachment, is limited to the short-wavelength region of excitation below 350 nm.

The infrared spectrum of **1b**, isolated in methane or other matrices, shows only three ν(CO) bands (Table 1) instead of the expected four (cf. **1a**, Fig. 1A); apparently, two of the vibrations are accidentally degenerate. In argon (Fig. 6) or methane matrices, selective irradiation (λ 365 nm) into the long-wavelength maximum of the electronic absorption spectrum of **1b** leads to the formation of a single new product, which exhibits one ν(CO) band (1898.5 in methane, 1903 cm^{-1} in argon). There is no indication of CO being liberated. This leads to the conclusion that this species contains an $Mo(CO)_4$ moiety with square planar geometry. Thus, we assign it as *trans*-$Mo(CO)_4(\eta^2$-NBD) (**7b**), bearing in mind that naked [29*] $Mo(CO)_4$ has a non-planar C_{2v} structure [39]. In the UV-visible spectrum we note a shoulder appearing at 260 nm and a moderate increase in the long-wavelength tail absorption from 400–600 nm. Subsequent irradiation in the latter region (λ 546 nm)

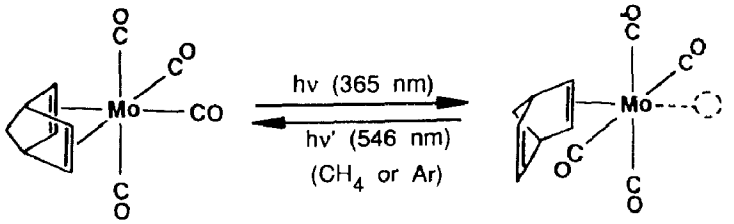

1b **7b** (6)

results in rapid, and quantitative, recovery of **1b**, eq. 6. This observation provides further support for the identity of **7b**, viz., that the norbornadiene ligand is still coordinated to the metal. The reaction can be driven forwards and backwards simply by changing the wavelength of irradiation (Fig. 6). However, the **1b** → **7b** conversion ceases when ca. 15% of **1b** have reacted, presumably because the system reaches a photostationary state which, at this wavelength, comprises 85% of **1b** and 15% of **7b**.

In a carbon monoxide matrix a similar irradiation at 365 nm converts **1b** into $Mo(CO)_6$ (1986.5 cm^{-1}) via the intermediate stage of $Mo(CO)_5(\eta^2$-NBD) (**4b**),

$$\mathbf{1b} \xrightarrow[\text{neat CO}]{\text{hv (365 nm)}} \underset{\mathbf{4b}}{Mo(CO)_5(\eta^2\text{–NBD})} + Mo(CO)_6 \qquad (7)$$

eq. 7, as indicated by the appearance of a weak band at 2078 cm^{-1} and a shoulder

at 1942 cm^{-1} on the lower frequency side of the strongest band of **1b**. While in neat CO no trace of the coordinatively unsaturated species **7b** could be detected, this species shows up in significant concentration when 365 nm irradiation of **1b** is performed in argon-diluted carbon monoxide (Ar/CO = 10/1). $Mo(CO)_6$ (1988 cm^{-1}) and **4b** appear as minor products, at least in the initial stages of the experiment. Noticeably, subsequent irradiation with λ 546 nm results in quantitative conversion of **7b** back to the starting material **1b**, but not in further production of $Mo(CO)_5(\eta^2$-NBD) (**4b**) and $Mo(CO)_6$, eq. 8 (L = CO).

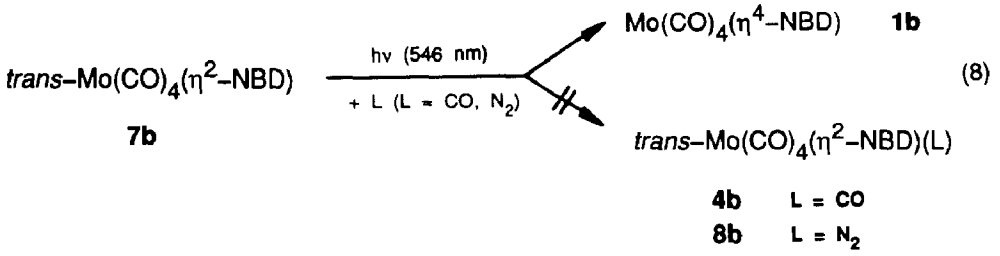

(8)

Similar behaviour of **7b** is observed in the presence of dinitrogen. Photolysis of **1b** with λ 365 nm in an Ar–N_2 (10/1) matrix generates **7b** as the major product (ca. 10% conversion after 1 min) together with a minor amount of a species exhibiting a weak ν(N≡N) vibration (2193 cm^{-1}) and one single ν(CO) band (1932.5 cm^{-1}), which is assigned to *trans*-$Mo(CO)_4(\eta^2$-NBD)(N_2) (**8b**). Subsequent irradiation with λ 546 nm leaves the concentration of **8b** unchanged while **7b** disappears completely with reformation of **1b**, eq. 8 (L = N_2). By contrast, 365 nm

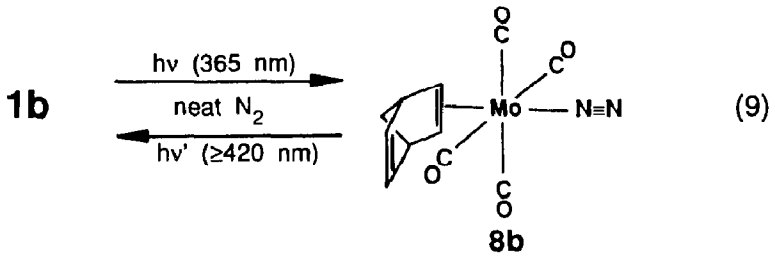

(9)

irradiation of **1b** in a neat dinitrogen matrix yields **8b** as the sole product, eq. 9, thus confirming the above assignment. This N_2 complex, upon irradiation through a 420 nm cut-off filter, decays slowly with partial recovery of **1b**.

In sharp contrast to the above results, short wavelength photolysis (λ 253 nm) of **1b** in either methane or argon matrices yields little, if any, *trans*-$Mo(CO)_4(\eta^2$-NBD) (**7b**). Instead, we note liberation of carbon monoxide together with the appearance of the characteristic three-band ν(CO) pattern of a *fac*-$M(CO)_3$ moiety (cf. Fig. 2B), thus providing clear evidence for the formation of *fac*-$Mo(CO)_3(\eta^4$-NBD) (**3b**) as the (almost) exclusive product, eq. 10. Even after 4 h of irradiation in argon (50% conversion of **1b**) no trace of the *mer* isomer **2b** could be detected, the high frequency band of which should appear around 2000 cm^{-1}. On the other hand, we cannot entirely exclude that a very minor proportion of **7b** remains undetected, bearing in mind the position of the single ν(CO) band of this species in close proximity to the strong absorptions of **1b** and **3b** around 1900 cm^{-1} (Table 1).

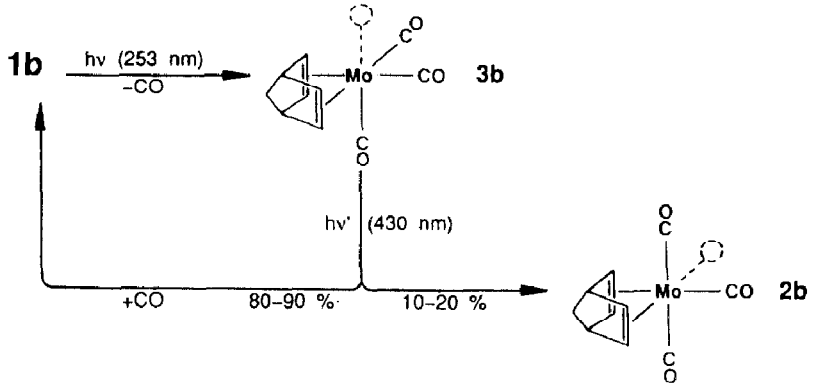

(10)

Unlike the analogous chromium species, **3b** does not undergo *fac* → *mer* rearrangement to more than a marginal extent. Instead, irradiation into the distinct electronic absorption maximum of **3b** near 430 nm results in efficient re-formation of **1b**, eq. 10. After 40 min 60% of **3b** has disappeared and the amount of regenerated **1b** accounts for more than 80% of this. There are some minor ν(CO) features which, by comparison with the analogous chromium species, are assigned to *mer*-$Mo(CO)_3(\eta^4$-NBD) (**2b**) and which should account for the rest of converted **3b**.

Not unexpectedly, photolysis of **1b** at λ 313 nm, i.e., at a wavelength halfway between those used in the above experiments, yields a mixture of both products, **3b** and **7b**. Again, the *mer* species **2b** is not observed as a primary photoproduct.

In the presence of N_2, loss of axial CO again is the predominant, if not exclusive, photolytic process of **1b** occurring upon electronic excitation at 253 nm. After 2 h of irradiation in a neat dinitrogen matrix, ca. 20% of **1b** has been converted into *fac*-$Mo(CO)_3(\eta^4$-NBD)(N_2) (**6b**), eq. 11, which is identified on the basis of its high-frequency ν(N≡N) vibration and the ν(CO) intensity pattern, indicative of a *fac*-$M(CO)_3$ skeleton (Table 1). An analogous photolysis in an Ar–N_2 (10/1) matrix yields mainly the corresponding unsaturated fragment **3b** (Table 1), which upon

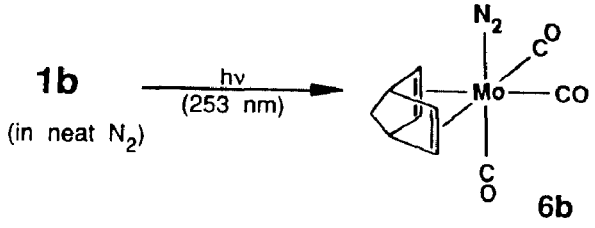

(11)

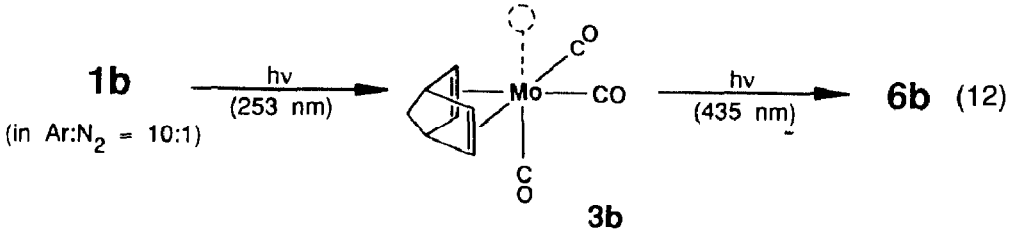

(12)

subsequent irradiation with λ 435 nm undergoes nearly quantitative conversion into the N_2 complex **6b**, eq. 12.

In a neat CO matrix, extended irradiation of **1b** at 253 nm results in slow formation of $Mo(CO)_6$ (40% conversion in 17 h). The axially vacant species **3b** shows up in moderate quantities when the 253 nm photolysis of **1b** is performed in an Ar–CO (10/1) matrix (Table 1), but disappears immediately upon subsequent irradiation into its electronic absorption maximum near 430 nm, which results in recovery of the starting material (**1b**) and formation of some $Mo(CO)_6$. These observations are in accord with the above finding that loss of CO from the axial position is the predominant photoprocess at 253 nm, however, when carbon monoxide is present in a large excess, it is very efficiently re-coordinated.

*Photolysis of $W(CO)_4(\eta^4$-norbornadiene) (**1c**)*

Regardless of the wavelength of excitation (253, 289, and 365 nm) the tungsten complex **1c** shows only one type of photoreaction: loss of an axial CO group with formation of *fac*-$W(CO)_3(\eta^4$-NBD) (**3c**; Table 1). Subsequent irradiation at the electronic absorption maximum of **3c** near 435 nm (where **1c** is almost transparent) results in partial re-formation of starting material. On this occasion the *mer* isomer **2c** appears in very minor concentration (2009 and 1946 cm^{-1}), which is barely detectable.

In a carbon monoxide matrix, the photolytic behaviour of **1c** resembles that of the analogous chromium and molybdenum complexes. Again, we observe stepwise substitution of the two C=C units of the norbornadiene ligand by carbon monoxide, yielding $W(CO)_5(\eta^2$-NBD) (**4c**; Table 1) in moderate stationary concentration and, ultimately, $W(CO)_6$ (1981.5 cm^{-1}). After 10 min irradiation at 365 nm ca. 25% conversion has been achieved, thus indicating that the efficiency of photolytic metal–diene bond cleavage compares well with that of CO photodissociation.

Dinitrogen is distinctly less effective than CO in trapping the $W(CO)_4(\eta^2$-NBD) primary photoproduct. It is only at the initial stages of the 365 nm photolysis of **1c** in a neat N_2 matrix that we note the appearance of *trans*-$W(CO)_4(\eta^2$-NBD)(N_2) (**8c**; Table 1), albeit in a minor concentration. Apart from this, almost exclusive conversion of **1c** into *fac*-$W(CO)_3(\eta^4$-NBD)(N_2) (**6c**; Table 1) is observed, which in higher concentration, after a longer period of irradiation, hides the minor ν(CO) feature associated with **8c**. Subsequent irradiation at λ 435 nm yields a slightly higher percentage of **8c**, but still **6c** is by far predominant.

Discussion

The photochemistry of $M(CO)_4(\eta^4$-NBD) complexes (M = Cr, Mo, W) involves both loss of CO and (partial) detachment of the diene ligand from the metal centre, eq. 13, but to a degree varying with the metal and the wavelength of excitation. In many respects the above results in low-temperature matrices broadly agree with complementary observations made in liquefied noble gases [22,23,40] and by means of time-resolved infrared detection of short-lived species [22,23].

The $\eta^4 \rightarrow \eta^2$ dechelation of the norbornadiene ligand is clearly observable in the case of the molybdenum complex **1b** upon selective long-wavelength irradiation (λ 365 nm) in various low-temperature matrices. However, instead of the expected [5,12,14] *cis*-vacant $Mo(CO)_4(\eta^2$-NBD) fragment of type **9**, an isomeric species, **7b**,

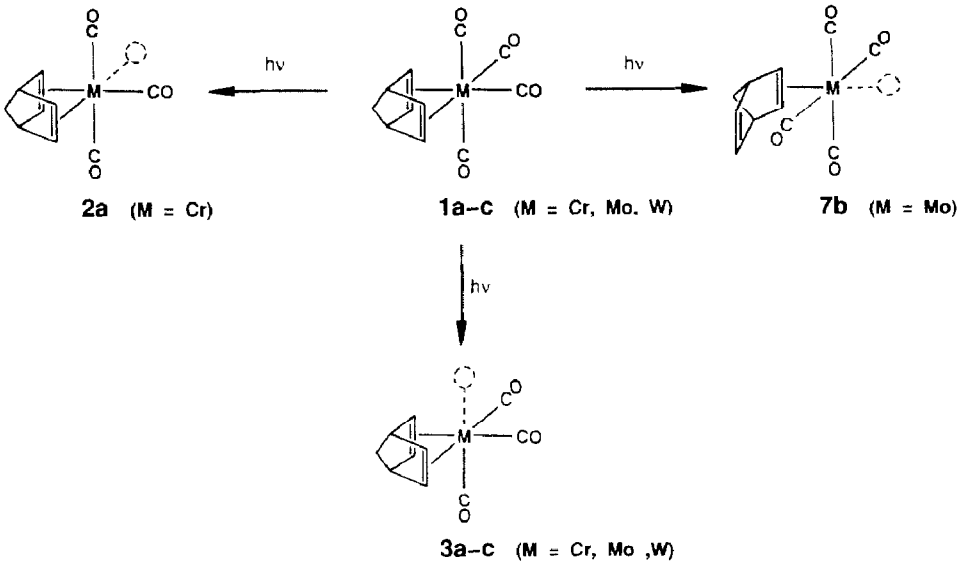

(13)

Scheme 1. Observed primary photoproducts of **1a–1c**.

is formed with a square planar $Mo(CO)_4$ moiety and, consequently, the vacant coordination site trans to the η^2-NBD ligand. In other words, photolytic norbornadiene $\eta^4 \rightarrow \eta^2$ dechelation is accompanied by skeletal $Mo(CO)_4$ rearrangement. We interpret this in terms of an excited-state isomerization of the *cis*-vacant five-coordinate species **9b** (Fig. 7) passing through an intermediate trigonal-bipyramidal geometry (**10b**) from which decay to the ground state of either

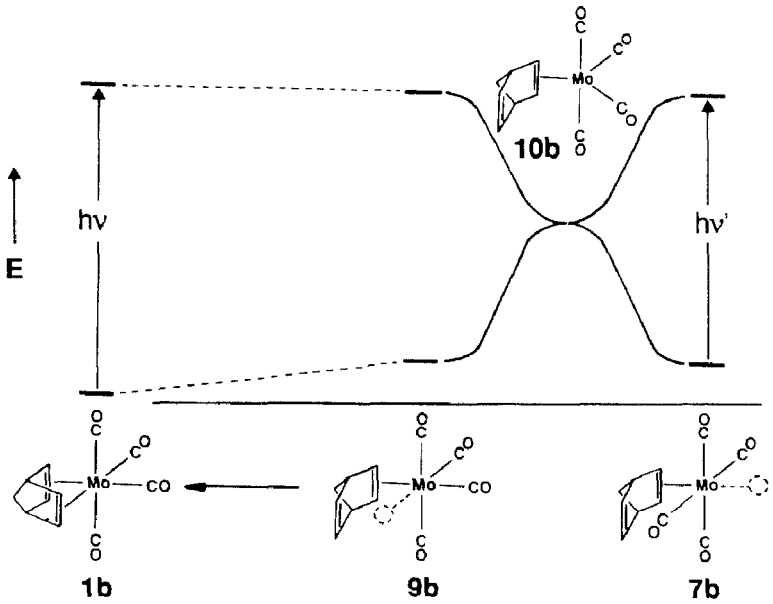

Fig. 7. A qualitative state diagram for the photochemical interconversion of $Mo(CO)_4(\eta^4$-NBD) (**1b**) and *trans*-vacant $Mo(CO)_4(\eta^2$-NBD) (**7b**), involving excited-state *cis*/*trans*-$Mo(CO)_4(\eta^2$-NBD) rearrangement.

$Mo(CO)_4(\eta^2\text{-NBD})$ isomer, **7b** or **9b**, should be possible. A similar excited-state rearrangement has been postulated for matrix isolated $M(CO)_5$ and $M(CO)_4(CS)$ fragments [41,42] in order to interpret the photo-induced pseudorotation of the former and the photochemical formation of various $W(CO)_3(^{13}CO)(CS)$ isomers from *trans*-$W(CO)_4(^{13}CO)(CS)$. The scheme shown in Fig. 7 contrasts with calculations on $Mo(CO)_4(\eta^2\text{-ethene})$ in so far that the *trans*-vacant isomer of this five-coordinate fragment, in both the excited and ground states, was predicted to be unstable towards rearrangement to the trigonal-bipyramidal structure and then further to the *cis*-vacant isomer [43,44]. However, as a matter of fact, the *trans*-vacant species **7b** is the only product detectable after 365 nm irradiation of **1b** in inert matrices, and the scheme shown in Fig. 7 provides the most simple rationalization of this finding.

Concerning the elusive *cis*-vacant fragment of type **9** we suspect that it decays immediately, even under low-temperature matrix conditions, with $\eta^2 \rightarrow \eta^4$ rechelation of the norbornadiene ligand, and that it therefore is neither directly detected nor trapped by taking up a potential ligand from the matrix environment. This would account for the very efficient and quantitative regeneration of the starting material **1b** upon selective long-wavelength excitation of **7b**, not only in an inert matrix environment, but also in N_2- and CO-doped argon matrices. Even in a neat N_2 matrix, where 365 nm excitation of **1b** yields *trans*-$Mo(CO)_4(\eta^2\text{-NBD})(N_2)$ (**8b**) in an appreciable amount, there is no evidence for *cis*-$Mo(CO)_4(\eta^2\text{-NBD})(N_2)$ formation as a result of N_2 coordination to the *cis*-vacant $Mo(CO)_4(\eta^2\text{-NBD})$ fragment. By analogy, we assume that this species is not involved in the initial step of norbornadiene displacement in **1b** by carbon monoxide. Instead, it should be the *trans*-vacant isomer **7b** which takes up CO, eq. 14, provided that this is available in a suitable orientation relative to the vacant coordination site. Otherwise, coordinatively unsaturated **7b** will be left behind, as it happens to occur in a matrix containing CO diluted with argon, and subsequent electronic excitation leads back to the starting material **1b**.

With these results in mind we consider it rather unlikely that a species of type **9** could be involved in the photocatalytic hydrogenation of norbornadiene by taking up H_2 at the *cis*-vacant coordination site, followed by hydrogen transfer to the diene to form norbornene [5,12,14]. This should apply particularly to the chromium and tungsten systems, since in these cases neither a *cis*- nor a *trans*-vacant $M(CO)_4(\eta^2\text{-NBD})$ species (**9** or **7**) has been observed. However, with regard to the conversion of **1a** or **1c** into the respective hexacarbonyl complexes it seems probable that a species of type **7** is involved in the initial step, i.e., the mechanism outlined in eq. 14 should be valid not only for molybdenum but also for chromium [38*] and tungsten.

Photolytic loss of CO is a process common to the complexes **1** of all three metals, eq. 13. In the cases of molybdenum and tungsten it involves exclusively the axial CO groups. This finding parallels the previous observation that in solution photoinduced ^{13}CO incorporation occurs selectively into the axial CO positions of **1b** and **1c** [12,18]. For the chromium complex **1a** the direction of ^{13}CO incorporation in solution could not be accurately assessed [12], but it was suggested to be analogous to that observed for the molybdenum and tungsten compounds. However, the photolytic behaviour of **1a** in low-temperature matrices shows clearly that CO photodetachment involves both the axial and the equatorial positions, followed by take-up of N_2 or ^{13}CO at the respective vacant coordination site. Notably, CO

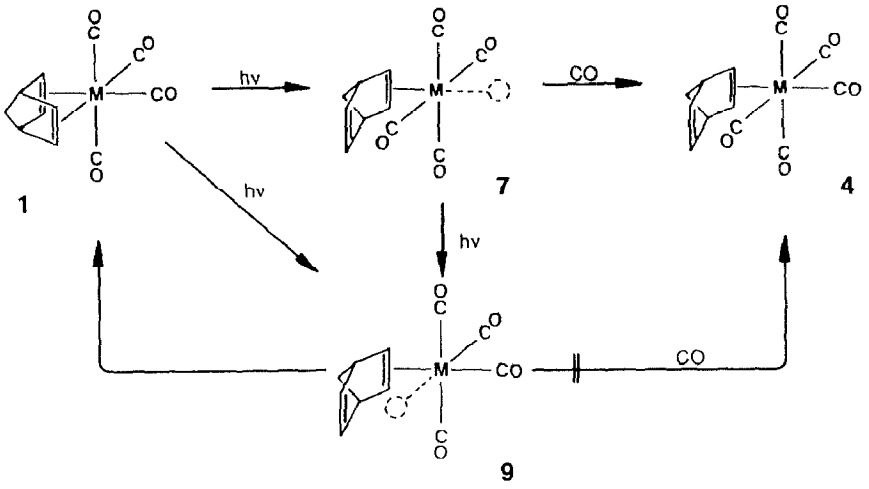

(14)

Scheme 2. Reactions proposed for the dechelation fragments 7 and 9.

photo-detachment from an equatorial position of **1a** is even predominating in the whole range of excitation at $\lambda \geqslant 289$ nm. This is difficult to rationalize since, estimating the metal–CO bond strengths from the degree of metal(d_π) → CO(π^*) back donation on the basis of the CO force constants [12,45] (cf. Table 2), one would expect the equatorial CO groups to be more strongly bound to the metal than the axial ones. Admittedly, such parameters represent ground state, not excited state properties, but in a similar context it has been suggested that the qualitative ordering of metal–carbon bond strength should be maintained [46].

The photochemical formation of equatorially substituted *mer*-M(CO)$_3$(η^4-NBD)(η^2-olefin) derivatives [21,47] is in apparent contrast with the selective axial CO photodetachment from **1b** and **1c**. However, at least in the case of the tungsten complex we have demonstrated [47] that the substitution of CO by the olefin initially occurs in the axial position, followed by *fac* → *mer* isomerization of the M(CO)$_3$(η^4-NBD)(η^2-olefin) product.

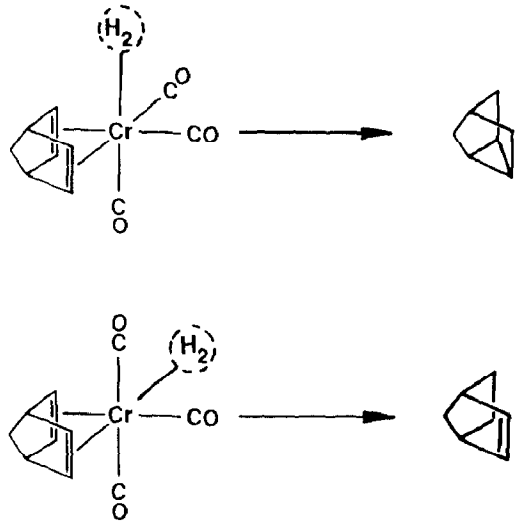

(15)

Regarding the photocatalytic diene hydrogenation we suspect that the $M(CO)_3$ moiety serves as the repeating unit in the catalytic cycle. Photogenerated $M(CO)_3(\eta^4$-NBD) should take up hydrogen, which then is transferred to the diene onto either the 1,4 or the 1,2 carbon atoms. The photolytic generation of both *mer*- and *fac*-$Cr(CO)_3(\eta^4$-NBD) fragments may thus explain, at first sight, why norbornadiene yields two hydrogenation products, norbornene and nortricyclene (eq. 15), while in case of a conjugated diene the exclusive *cis*-1,4-hydrogenation coincides with the selective axial CO photodetachment from $Cr(CO)_4(\eta^4$-1,3-diene) [17]. However, we must not fail to notice that the molybdenum and tungsten complexes **1b** and **1c**, losing CO from the axial position, in the photocatalytic process produce both norbornene and nortricyclene, the former predominating in the case of molybdenum and the latter in the case of tungsten [12]. Thus, one particular lesson to be drawn from this study is that even reliable information on primary products or other species involved in a catalytic system should be taken with a grain of salt, when expanding on detailed mechanistic implications. With regard to the particular case of photocatalytic diene hydrogenation we have to consider the possibility that reversible *fac* ⇄ *mer* rearrangement of the $M(CO)_3$ moiety, subsequent to the initial photolytic formation of the $M(CO)_3(\eta^4$-NBD) fragment, is an integral part of the catalytic process [23,33*].

Acknowledgement

We are indebted to Mrs. G. Klihm for skilled technical assistence and to Dipl.-Chem. D. Chmielewski for the preparation of ^{13}CO-enriched $Cr(CO)_4(\eta^4$-NBD). Fruitful discussions with Dr. M. Poliakoff and Prof. J.J. Turner (University of Nottingham, U.K.) and support of this work within the framework of the EEC Stimulation Grants ST2J-0081-2-C(CD) and SC1*007-C(EDB) are gratefully acknowledged. We also thank the S.E.R.C. for a studentship (to R.H.H.) and for support (to A.J.R.).

References

1 Preliminary accounts on parts of this work have been given at the XIIth IUPAC Symposium on Photochemistry, Bologna/Italy, Sept. 1988 (F.-W. Grevels, J. Jacke, W.E. Klotzbücher, S. Özkar, V. Skibbe, Pure Appl. Chem., 60 (1988) 1017) and at the XIth International Conference on Organometallic Chemistry, Callaway Gardens, Pine Mountain/Georgia, U.S.A., Oct. 1983 (R.H. Hooker; A.J. Rest).
2 J. Nasielski, P. Kirsch, L. Wilputte-Steinert, J. Organomet. Chem., 27 (1971) C13.
3 G. Platbrood, L. Wilputte-Steinert, Bull. Soc. Chim. Belg., 82 (1973) 733.
4 M. Wrighton, M.A. Schroeder, J. Am. Chem. Soc., 95 (1973) 5764.
5 G. Platbrood, L. Wilputte-Steinert, J. Organomet. Chem., 70 (1974) 393.
6 G. Platbrood, L. Wilputte-Steinert, Tetrahedron Lett., (1974) 2507.
7 G. Platbrood, L. Wilputte-Steinert, J. Organomet. Chem., 70 (1974) 407.
8 M.S. Wrighton, M.A. Schroeder, J. Am. Chem. Soc., 96 (1974) 6235.
9 M.S. Wrighton, D.S. Ginley, M.A. Schroeder, D.L. Morse, Pure Appl. Chem., 41 (1975) 671.
10 G. Platbrood, L. Wilputte-Steinert, J. Mol. Cat., 1 (1975/76) 265.
11 I. Fischler, M. Budzwait, E.A. Koerner von Gustorf, J. Organomet. Chem., 105 (1976) 325.
12 D.J. Darensbourg, H.H. Nelson, III, M.A. Murphy, J. Am. Chem. Soc., 99 (1977) 896.
13 M.J. Mirbach, D. Steinmetz, A. Saus, J. Organomet. Chem., 168 (1979) C13.
14 M.J. Mirbach, T.N. Phu, A. Saus, J. Organomet. Chem., 236 (1982) 309.
15 M.A. Schroeder, M.S. Wrighton, J. Organomet. Chem., 74 (1974) C29.
16 M. Cais, A. Rejoan, Inorg. Chim. Acta, 4 (1970) 509.
17 W. Gerhartz, F.-W. Grevels, W.E. Klotzbücher, E.A. Koerner von Gustorf, R.N. Perutz, Z. Naturforsch. B, 40 (1985) 518.

18 D.J. Darensbourg, H.H. Nelson, III, J. Am. Chem. Soc., 96 (1974) 6511.
19 G. Platbrood, L. Wilputte-Steinert, J. Organomet. Chem., 85 (1975) 199.
20 D. Rietvelde, L. Wilputte-Steinert, J. Organomet. Chem., 118 (1976) 191.
21 F.-W. Grevels, J. Jacke, P. Betz, C. Krüger, Y.-H. Tsay, Organometallics, 8 (1989) 293.
22 S.A. Jackson, P.M. Hodges, M. Poliakoff, J.J. Turner, F.-W. Grevels, J. Am. Chem. Soc., accepted for publication.
23 P.M. Hodges, S.A. Jackson, J. Jacke, M. Poliakoff, J.J. Turner, F.-W. Grevels, J. Am. Chem. Soc., accepted for publication.
24 W. Gerhartz, F.-W. Grevels, W.E. Klotzbücher, Organometallics, 6 (1987) 1850.
25 W.E. Klotzbücher, Cryogenics, 23 (1983) 554.
26 H. Werner, P. Prinz, Chem. Ber., 100 (1967) 265.
27 R.B. King, A. Fronzaglia, Inorg. Chem., 5 (1966) 1837.
28 K.R. Pope, M.S. Wrighton, Inorg. Chem., 24 (1985) 2792.
29 There is accumulating evidence for vacant coordination sites being occupied by matrix host atoms or molecules (e.g., R.N. Perutz, J.J. Turner, J. Am. Chem. Soc., 97 (1975) 4791), as pointed out by a referee. However, since this paper is not aimed at the investigation of such specific interactions, for the sake of simplicity we prefer the notation of the fragment species as coordinatively unsaturated complexes rather than to formulate them as "solvates".
30 P.S. Braterman, Metal Carbonyl Spectra, Academic Press, London, 1975.
31 H. Angermund, F.-W. Grevels, R. Moser, B. Benn, C. Krüger, M.J. Romão, Organometallics, 7 (1988) 1994.
32 Various square-pyramidal $LM(CO)_4$ fragments existing in two isomeric forms have been reported to undergo photochemical interconversion in low-temperature matrices: (a) J.D. Black, P.S. Braterman, J. Organomet. Chem., 63 (1973) C19; (b) S.P. Church, M. Poliakoff, J.A. Timney, J.J. Turner, Inorg. Chem., 22 (1983) 3259; (c) A. Horton-Mastin; M. Poliakoff, J.J. Turner, Organometallics, 5 (1986) 405; (d) cf. ref. 42.
33 *mer*-$Cr(CO)_3(\eta^4\text{-NBD})(\eta^2\text{-ethene})$ undergoes facile substitution of ethene by other ligands. The product obtained from the reaction with ^{13}CO contains both of the two mono-(^{13}CO)-labelled derivatives of **1a**, $Cr(CO)_3(ax\text{-}^{13}CO)(\eta^4\text{-NBD})$ and $Cr(CO)_3(eq\text{-}^{13}CO)(\eta^4\text{-NBD})$, as well as ca. 50% unlabelled **1a** resulting from partial self-decomposition of the ethene complex. Formation of bis(^{13}CO)-labelled **1a** is negligible. D. Chmielewski, F.-W. Grevels, J. Jacke, in preparation.
34 Our result $k_{ax,ax} < k_{eq,eq}$ agrees with literature data for M = Mo [12,45] and W [12,18,45], but contradicts with literature data for M = Cr [12,45] and with the general assumption $k_{trans} \approx 2k_{cis}$ for substituted group 6 metal carbonyls (F.A. Cotton, C.S. Kraihanzel, J. Am. Chem. Soc., 84 (1962) 4432).
35 F.-W. Grevels, V. Skibbe, J. Chem. Soc., Chem. Commun., (1984) 681.
36 V. Skibbe, Doctoral Dissertation, MPI für Strahlenchemie, Universität Duisburg (FRG), 1985.
37 I.W. Stolz, G.R. Dobson, R.K. Sheline, Inorg. Chem., 2 (1963) 1264.
38 An attempt was made to identify the position of the incoming CO group by generating ^{13}CO-labelled **4a** in an analogous experiment involving irradiation of **1a** with $\lambda \geq 435$ nm in a neat ^{13}CO matrix. The appearance of only one high-frequency $\nu(CO)$ band (2065 cm^{-1}, red-shifted from the corresponding band of unlabelled **4a** by 3 cm^{-1}) indicates that a single ^{13}CO-labelled product is formed. However, the spectral changes in the lower-frequency $\nu(CO)$ region did not allow an unambiguous assignment to a particular $Cr(CO)_4(^{13}CO)(\eta^2\text{-NBD})$ isotopomer with the ^{13}CO group either in the *trans*- or a *cis*-position to the η^2-NBD ligand.
39 R.N. Perutz, J.J. Turner, J. Am. Chem. Soc., 97 (1975) 4800.
40 (a) R.R. Andréa, D.J. Stufkens, A. Oskam, personnal communication; (b) R.R. Andréa, Doctoral Dissertation, Universiteit van Amsterdam, 1989.
41 J.K. Burdett, J.M. Grzybowski, R.N. Perutz, M. Poliakoff, J.J. Turner, R.F. Turner, Inorg. Chem., 17 (1978) 147.
42 M. Poliakoff, Inorg. Chem., 15 (1976) 2892.
43 C. Daniel, A. Veillard, Nouv. J. Chim., 10 (1986) 83.
44 A. Veillard, C. Daniel, A. Strich, Pure Appl. Chem., 60 (1988) 215.
45 D.J. Darensbourg, J.E. Tappan, H.H. Nelson, III, Inorg. Chem., 16 (1977) 534.
46 R.M. Dahlgreen, J.I. Zink, Inorg. Chem., 16 (1977) 3154.
47 (a) F.-W. Grevels, J. Jacke, in preparation; (b) J. Jacke, Doctoral Dissertation, MPI für Strahlenchemie, Universität Duisburg (FRG), 1989.